

# High-statistics finite size scaling analysis of U(1) lattice gauge theory with Wilson action

Burkhard Klaus

*Institut für Theoretische Physik, Freie Universität Berlin, D-14195 Berlin, Germany  
 and DESY-IfH Zeuthen, D-15735 Zeuthen, Germany*

Claude Roiesnel

*Centre de Physique Théorique, Centre National de la Recherche Scientifique, UPR A0014,  
 Ecole Polytechnique, 91128 Palaiseau Cedex, France  
 (December 1997)*

We describe the results of a systematic high-statistics Monte-Carlo study of finite-size effects at the phase transition of compact U(1) lattice gauge theory with Wilson action on a hypercubic lattice with periodic boundary conditions. We find unambiguously that the critical exponent  $\nu$  is lattice-size dependent for volumes ranging from  $4^4$  to  $12^4$ . Asymptotic scaling formulas yield values decreasing from  $\nu(L \geq 4) \approx 0.33$  to  $\nu(L \geq 9) \approx 0.29$ . Our statistics are sufficient to allow the study of different phenomenological scenarios for the corrections to asymptotic scaling. We find evidence that corrections to a first-order transition with  $\nu = 0.25$  provide the most accurate description of the data. However the corrections do not follow always the expected first-order pattern of a series expansion in the inverse lattice volume  $V^{-1}$ . Reaching the asymptotic regime will require lattice sizes greater than  $L = 12$ . Our conclusions are supported by the study of many cumulants which all yield consistent results after proper interpretation.

## I. INTRODUCTION

The U(1) lattice gauge model has been studied from the early days of numerical simulations of gauge theories [1]. Its apparent simplicity makes it a natural choice for testing concepts and techniques used in simulations of non-abelian lattice gauge theories. However it turned out that the abelian character of the U(1) model brings specific difficulties. It can be proven rigorously under rather general assumptions [2] that abelian lattice gauge theories have a phase transition at finite coupling though the order is not known. The determination by numerical simulations of the properties of the critical point in compact U(1) lattice gauge theory with Wilson action and periodic boundary conditions has been strongly dependent of the computing power available at the time.

The early simulations [3] made runs with a few hundred iterations at each coupling constant on rather small ( $4^4$  to  $6^4$ ) lattices. They reported a second-order phase transition but observed some signs of metastability with longer runs at isolated points. Subsequent simulations [4]

made runs with a few thousand iterations on larger ( $8^4$  up to  $16^4$ ) lattices. It became possible to histogram the runs and to observe a gap in the plaquette energy. They concluded to the existence of a first-order critical point but did notice a decrease of the gap with the lattice size which was later confirmed [5] on  $9^4$  and  $(3\sqrt{3})^4$  lattices.

But the situation became still more confusing in the following years. Indeed the results, always for lattices with periodic boundary conditions and with runs of  $O(10^4)$  length, have usually depended on which method was used for studying the phase transition. Most studies using the Monte-Carlo renormalization group transformation [6–9] have claimed a second order phase transition, but sometimes with very different critical exponents, whereas most works based on finite size scaling theory [10–12] have concluded to a first-order transition, but again with a critical exponent not consistent with the first-order prediction. These discrepancies led the subject into an expectant state.

The interest about the nature of the phase transition has been revived more recently by two new kinds of results. The role played by topological excitations, the monopoles, had been the object of inquiries since the very beginning of numerical studies of the U(1) lattice gauge theory [13]. The influence of topology on the critical properties can be probed in several ways. One approach [14–17] is to add to the standard Wilson action a coupling  $\lambda$  controlling the density of monopoles. There is some evidence [18] in favor of the existence of a non-gaussian second-order critical point in the  $(\beta, \lambda)$  plane when monopoles are suppressed. There is also preliminary evidence [19] against universality with respect to  $\lambda$ . Another approach [20,21] is to study the compact U(1) gauge theory on lattices with sphere-like topology with a Wilson action extended by a coupling  $\gamma$  of charge 2

$$S = \beta \sum_P \cos \Theta_P + \gamma \sum_P \cos 2\Theta_P \quad (1)$$

No signs of metastability are found on these lattices for  $\gamma \leq 0$ . A finite-size scaling analysis of the data on sphere-like lattices [22] has concluded to the existence, for  $\gamma \leq 0$ ,

of a second-order transition with a non-gaussian continuum limit. However we must notice that the critical exponents of these two approaches are still different.

The latter result has spawned further investigations. There has been a study [23] of the scaling behaviour of gauge-ball masses and of the static potential, which claims to confirm the second-order nature of the transition also on lattices with periodic boundary conditions at  $\gamma = -0.2$  and  $\gamma = -0.5$  with a critical exponent  $\nu \approx 0.36$  consistent with universality and the finite-size scaling analysis of sphere-like lattices. The results on lattices with spherical topology could also lend support to the suspicion that the first-order signal observed on toroidal lattices might be a finite-size effect due to the topology of the lattice. This suspicion had been raised by the observation of the decrease of the gap mentioned above. However the measurements of gaps were not accurate enough and systematic enough to make a statement about the infinite volume limit. The particular case of the Wilson action was therefore re-investigated [24,25] with increased statistics ( $O(10^5)$  for each coupling constant) and an emphasis on the study of gaps. There was definite evidence that the latent heat extrapolates to a non-zero value in the infinite volume limit of toroidal lattices. Moreover the measurement of the critical exponent,  $\nu \approx 0.33$ , though clearly different from the first-order prediction, was not statistically consistent with the claim of universality with respect to the coupling  $\gamma$ .

Therefore there is always an apparent contradiction between the simulations on lattices with sphere-like topology and on lattices with periodic boundary conditions since one observes a gap on the latter even when  $\gamma < 0$ . Moreover the dispersion of the predicted values for the critical exponent  $\nu$  is always as large as before, despite the increase in statistics since the last decade. One can fairly state that the confusion about the nature of the transition has also increased! But one can now strongly suspect that the origin of these paradoxical results could be explained by the presence of systematic corrections to the asymptotic finite-size scaling formulas. This will be our working hypothesis. There are two ways of circumventing these corrections. The most straightforward approach is to simulate the largest possible lattices for a given computing power. However, for a transition with a weak first-order signal like U(1), one must thoroughly assess whether the number of tunnelling events is sufficient to get statistically reliable results. The other approach is to perform a finite-size scaling analysis of the four-dimensional compact U(1) gauge theory on smaller lattices but with the same quality standard as the best analyses of three-dimensional spin models. Such an analysis must meet two criteria. On the one hand the simulation must be done on many lattice sizes (and not restricted to 3 or 4 data points as is so often the case) in order to be able to test the *stability* of the fits. On the other hand the statistics must be large enough to *disentangle* the systematic errors from the statistical errors. Only then can we interpret correctly the observed deviations in a crit-

ical exponent extracted from different observables. We can learn from the two and three dimensional numerical studies of spin models how large the statistics must be: one needs at least  $O(10^6)$  configurations at each coupling constant. None of the presently published studies of the U(1) phase transition satisfy both constraints and we contend that this is the source of the contradictory results.

The purpose of this work is to present a study at eight lattice sizes with statistics up to  $O(10^7)$  at each pseudo-critical coupling after reweighting and to clarify the nature of the U(1) phase transition. In the next section we shall review the part of finite-size scaling theory that we shall need in the sequel to interpret the data. Then we shall describe the details of our Monte-Carlo simulation and present the results of the measurements. In the following sections we shall discuss, for various cumulants, the finite-size scaling analysis of their pseudo-critical couplings and of their extrema. The conclusion will be devoted to putting all these results into a coherent perspective.

## II. FRAMEWORK OF THE FINITE-SIZE SCALING ANALYSIS

### A. Scaling ansatz

Most of the numerical finite-size scaling analyses of the phase transition in the U(1) lattice gauge theory have been restricted to the specific-heat and the Binder cumulant. When scaling violations are important, as it turns out for U(1), introducing higher-order cumulants brings some improvement as we shall explain below. Most reviews on finite-size scaling theory discuss the magnetic cumulants only. Studying energy cumulants carries some specific features. Even if this is standard lore we shall briefly remind some useful formulas not always easy to find elsewhere. First, to fix our notations, we recall that the canonical partition function of a lattice gauge theory on a  $d$ -dimensional cubic lattice of size  $L$  can be written as

$$Z(\beta, L) = \int \Omega(E, L) e^{-\beta V E} dE \quad (2)$$

$$= e^{-V F(\beta, L)} \quad (3)$$

where  $\Omega(E, L)$  is the microcanonical partition function,  $E$  is the plaquette energy and the volume, for a lattice gauge theory, is  $V = \frac{1}{2}d(d-1)L^d$ .

Standard arguments [26] lead for continuous phase transitions to the free energy density decomposition in a singular part and an analytic contribution:

$$F(\beta, L) = L^{-d} f_0(x) + f_{ns}(t, L) \quad (4)$$

where  $x = |t|L^{\frac{1}{\nu}}$  is the scaling variable and  $t = \frac{\beta}{\beta_c} - 1$  is the reduced coupling. In this parameterization, the

hyperscaling relation  $\alpha = 2 - \nu d$  is assumed with only one relevant scaling variable  $x$  and no dangerous irrelevant variable. Moreover one assumes that there are no marginal variables and no logarithmic bulk singularities, even if we work in dimension  $d = 4$ , which could be the upper critical dimension of the continuum limit if there were a second-order phase transition.

The function  $f_{ns}$  represents the non-singular contribution of the background to the free energy density.  $f_{ns}(t, L)$  is an analytic function in  $t$ . Its dependence upon  $L$  is not so clear. There is a conjecture [27] that for periodic systems one can take  $f_{ns}(t, L) \approx f(t, \infty)$ . We shall assume that this conjecture holds true and that the  $L$ -dependence is exponentially suppressed:

$$f_{ns}(t, L) = f_{00} + f_{01}t + f_{02}t^2 + \dots + O\left(e^{-L/\xi}\right) \quad (5)$$

However one must be aware that for systems with free boundary conditions one expects in general that  $F(\beta, L)$  can have geometrical terms present, which are proportional to inverse integral powers of  $1/L$ .

There are further analytic corrections introduced by non-linearities in the scaling variables away from criticality either when solving the renormalization group beyond the linear approximation,  $t' = t + O(t^2)$ , or for instance, when using  $t' = \beta_c/\beta - 1$  instead of  $t$ . Expressing the non-linear scaling variable  $x' = t' L^{1/\nu}$  in terms of  $x$  yields corrections in powers of  $L^{-\frac{1}{\nu}}$ . We will neglect these corrections.

In the renormalization group description of second-order phase transitions, one expects corrections to the asymptotic scaling function  $f_0(x)$  induced by the irrelevant variables. We shall keep the leading contribution in these corrections and parameterize it by an exponent  $\omega > 0$ . Therefore we write

$$F(\beta, L) = L^{-d} (f_0(x) + L^{-\omega} f_1(x)) + f_{ns}(t) \quad (6)$$

We stress that this ansatz for the free energy density is a natural, but completely phenomenological generalization of the asymptotic scaling formula. Moreover this ansatz still depends at least upon 4 parameters. It is not yet possible to extract that many parameters from a numerical finite-size analysis. We will have to resort to further approximations and limit ourselves to considering three-parameter fitting ansätze.

Ansatz (6) can also describe the finite-size behavior at first-order transitions. Even if there is not so much known about this behavior from a theoretical standpoint, one usually expects [28] that  $\nu^{-1} = \omega = d$ . Heuristic arguments based on the double-gaussian approximation [29–31] predict that the corrections should be expressible as a power series in  $V^{-1}$ . These arguments can be put onto a rigorous basis [32–34] in the special case of q-states Potts models for large q.

## B. Standard cumulants

In principle we would better like to determine directly the finite-size scaling properties of  $\Omega(E, L)$  or equivalently of the probability distribution  $P(E, L)$  of the plaquette energy. In practice it is more convenient to extract the different moments of the plaquette distribution:

$$\langle E^n \rangle = \frac{(-1)^n}{V^n} \frac{1}{Z(\beta, L)} \frac{\partial^n Z}{\partial \beta^n} \quad (7)$$

$$\frac{\partial \langle E^n \rangle}{\partial \beta} = V (\langle E \rangle \langle E^n \rangle - \langle E^{n+1} \rangle) \quad (8)$$

Then, with ansatz (6) it is easy to derive the scaling properties of any cumulant from these moments. The choice of cumulants to include in the analysis is, in a large respect, rather arbitrary. Of course, for the sake of comparison with previous works, we have to study standard cumulants such as the specific heat:

$$C_v(\beta, L) = -\beta^2 \frac{\partial^2}{\partial \beta^2} F(\beta, L) \quad (9)$$

$$= \beta^2 V (\langle E^2 \rangle - \langle E \rangle^2) \quad (10)$$

and the Binder cumulant:

$$U_4(\beta, L) = \frac{1}{3} \left( 1 - \frac{\langle E^4 \rangle}{\langle E^2 \rangle^2} \right) \quad (11)$$

We shall also introduce the second cumulant:

$$U_2(\beta, L) = 1 - \frac{\langle E^2 \rangle}{\langle E \rangle^2} \quad (12)$$

These low-order cumulants are sensitive to the analytic contribution to the free energy density in Eq. (6). For instance ansatz (6) implies the following for the scaling behavior of the specific heat:

$$C_v(\beta, L) = -\frac{\beta^2}{\beta_c^2} L^{-d+\frac{2}{\nu}} (f_0''(x) + L^{-\omega} f_1''(x)) - 2f_{00} \frac{\beta^2}{\beta_c^2} \quad (13)$$

But we know that  $\frac{1}{d} \leq \nu \leq \frac{1}{2}$  and we can expect that  $\omega \approx \frac{2}{\nu} - d$ . Such an approximate equality would imply that the next-to-leading contribution comes both from the corrections to scaling and from the analytic background. Then we can anticipate difficulties in describing the scaling behavior of the specific heat with three-parameter ansätze.

In the same way the predicted finite-size scaling behavior of the second cumulant and the Binder cumulant is:

$$U_2(\beta, L) = L^{-2d+\frac{2}{\nu}} \left( u_{20}(x) + u_{21}(x) L^{-d+\frac{1}{\nu}} + O\left(L^{d-\frac{2}{\nu}}, L^{-2d+\frac{2}{\nu}}, L^{-\omega}\right) \right) \quad (14)$$

$$U_4(\beta, L) = L^{-2(d-\frac{1}{\nu})} \left( u_{40}(x) + u_{41}(x)L^{-(d-\frac{1}{\nu})} + O\left(L^{-2(d-\frac{1}{\nu})}, L^{d-\frac{2}{\nu}}, L^{-\omega}\right) \right) \quad (15)$$

The corrections to scaling are now governed by the exponent  $d - \frac{1}{\nu}$ . We can expect to run into problems describing these corrections when  $\nu \approx \frac{1}{d}$ . In the limit  $\nu = \frac{1}{d}$ , for first-order transitions, Eqs. (13,14,15) yield the correct leading behavior but the corrections become of order  $L^{-d}$ .

One can notice [35] that deriving Eqs. (13,14,15) with respect to  $\beta$  introduces an additional factor  $L^{\frac{1}{\nu}}$  through the scaling variable  $x$ . Therefore studying the finite-size scaling behavior of the derivatives of the standard cumulants should make it easier to determine the critical exponent  $\nu$ . We have also introduced these cumulants into our analysis:

$$\frac{\partial C_v}{\partial \beta} = V \left[ 2\beta \left( \langle E^2 \rangle - \langle E \rangle^2 \right) - \beta^2 V \left( \langle E^3 \rangle - 3 \langle E^2 \rangle \langle E \rangle + 2 \langle E \rangle^3 \right) \right] \quad (16)$$

$$\frac{\partial U_2}{\partial \beta} = \frac{V}{\langle E \rangle^3} \left( \langle E^3 \rangle \langle E \rangle + \langle E^2 \rangle \langle E \rangle^2 - 2 \langle E^2 \rangle^2 \right) \quad (17)$$

$$\frac{\partial U_4}{\partial \beta} = \frac{V}{3 \langle E^2 \rangle^3} \left( \langle E^5 \rangle \langle E^2 \rangle + \langle E^4 \rangle \langle E^2 \rangle \langle E \rangle - 2 \langle E^4 \rangle \langle E^3 \rangle \right) \quad (18)$$

In order to make a comparison between different lattice sizes one still needs a prescription to define a common value of the scaling variable  $x$ . One usually uses the location of an extremum of a cumulant  $\kappa(\beta, L)$  to define a universal value  $x_\kappa^*$ , independent of  $L$ . When there are several extrema it is natural to choose the extremum closest to the infinite volume critical point. Fig. 1 displays the plots of the cumulants  $C_v \times V^{-1}, U_4$  and their derivatives  $\frac{\partial C_v}{\partial \beta} \times V^{-1}, \frac{\partial U_4}{\partial \beta} \times V^{-1}$  as a function of  $\beta$  and which extremum we have studied in each case. They have been produced by reweighting a run with  $10^6$  iterations on a  $12^4$  lattice at  $\beta = 1.01024$ . We recall that the critical coupling of U(1) lattice gauge with Wilson action and periodic boundary conditions is  $\beta_c(\infty) \approx 1.011$ .

### C. Derivatives of the free energy density

We have just seen that it is not always easy to interpret the scaling corrections to the standard cumulants or their derivatives. The interpretation would be more tractable if we could study cumulants which are directly expressible in terms of the free energy. In particular we can

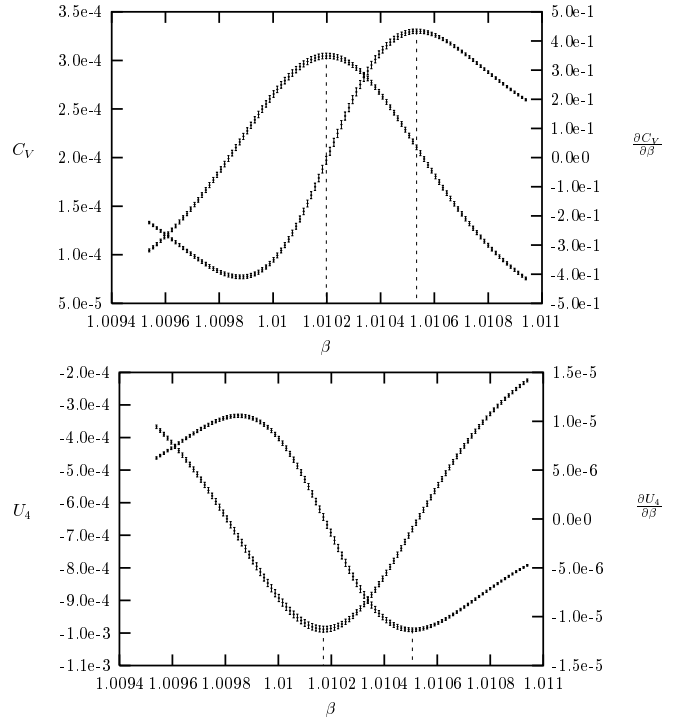


FIG. 1. The cumulants  $C_v \times V^{-1}, U_4$  and their derivatives  $\frac{\partial C_v}{\partial \beta} \times V^{-1}, \frac{\partial U_4}{\partial \beta} \times V^{-1}$  on a  $12^4$  lattice as a function of  $\beta$ .

introduce the energy cumulants  $\kappa_n(\beta, L)$  [36] which are defined through the Taylor expansion of the free energy density  $F(\beta, L)$ :

$$F(\beta', L) = F(\beta, L) - \sum_{n=1}^{\infty} \frac{(-1)^n}{n!} \kappa_n(\beta, L) (\beta' - \beta)^n \quad (19)$$

The finite-size scaling behavior of these energy cumulants is much simpler since they are simply the derivatives of the free energy density:

$$\begin{aligned} (-1)^{n+1} \kappa_n(\beta, L) &= \frac{\partial^n F(\beta, L)}{\partial \beta^n} \\ &= \frac{1}{\beta_c^n} L^{-d+\frac{n}{\nu}} \left( f_0^{(n)}(x) + L^{-\omega} f_1^{(n)}(x) \right) + f_{ns}^{(n)}(\beta) \end{aligned} \quad (20)$$

The analytic piece  $f_{ns}^{(n)}(\beta)$  can be neglected as soon as  $n \geq 3$ . The first three cumulants coincide with the central moments:

$$\kappa_1 = \langle E \rangle \quad (21)$$

$$\kappa_2 = V \left( \langle E^2 \rangle - \langle E \rangle^2 \right) = \mu_2 = C_v / \beta^2 \quad (22)$$

$$\kappa_3 = V^2 \left\langle (E - \langle E \rangle)^3 \right\rangle = \mu_3 \quad (23)$$

The higher-order cumulants can be expressed as non-linear combinations of the central moments  $\mu_n = V^{n-1} \langle (E - \langle E \rangle)^n \rangle$ . We shall introduce in our analysis the cumulants  $\kappa_n$  up to sixth order:

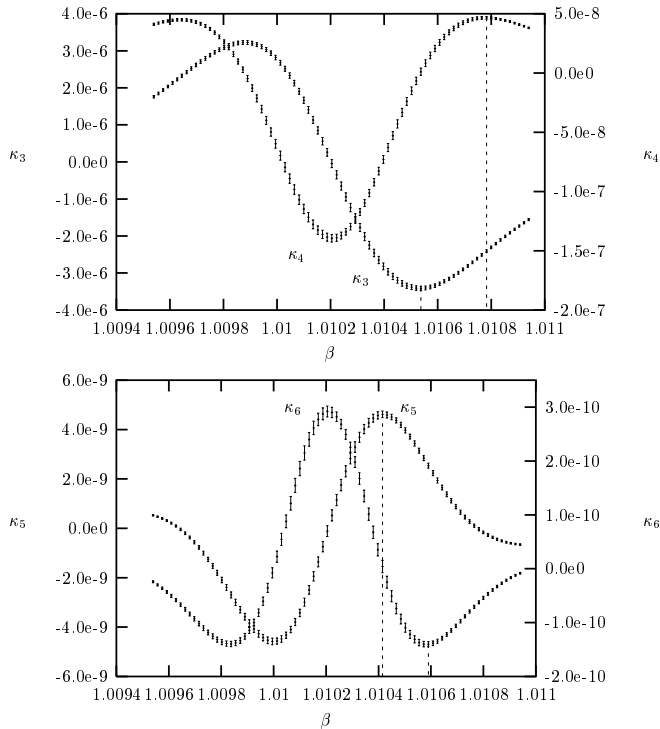


FIG. 2. The cumulants  $\kappa_n \times V^{-n+1}$  on a  $12^4$  lattice as a function of  $\beta$ .

$$\kappa_4 = \mu_4 - 3V\mu_2^2 \quad (24)$$

$$\kappa_5 = \mu_5 - 10V\mu_2\mu_3 \quad (25)$$

$$\kappa_6 = \mu_6 - 15V\mu_2\mu_4 - 10V\mu_3^2 + 30V^2\mu_2^3 \quad (26)$$

Fig. 2 displays the plots of the cumulants  $\kappa_n \times V^{-n+1}$  on a  $12^4$  lattice as a function of  $\beta$  and which extremum we have studied in each case.

These energy cumulants have not been studied very often in finite-size scaling analyses of phase transitions. In lower dimensions and for spin models the emphasis is of course on magnetic cumulants and the standard set of cumulants is natural in this context. The energy cumulants  $\kappa_n$  are more suitable to the analysis of four-dimensional field theories.

### III. SIMULATION DETAILS

Previous studies [24,25] provide us already with a good knowledge of the locations of pseudo-critical couplings at eight lattice sizes. We have therefore decided to increase the statistics at several couplings inside the error bars of these pseudo-critical points. For each coupling we did at least two runs with hot and cold starts, different random generators with large periods, and statistics of  $5 \cdot 10^5$  configurations. For a complete overview of our statistics we refer to Table I. The simulated  $\beta$ -values are quite close to each other and we can use the spectral density

L	$\beta$	iterations	L	$\beta$	iterations
4	0.9785	$5 \times 10^6$	5	0.9940	$12 \times 10^6$
	0.9795			0.9952	
6	1.0014	$7 \times 10^6$	7	1.0052	$4 \times 10^6$
	1.0020			1.0055	
8	1.0072	$5.5 \times 10^6$	9	1.0084	$4.5 \times 10^6$
	1.0076			1.0088	
10	1.0092	$1 \times 10^6$	12	1.0101	$1 \times 10^6$
	1.0093	$1 \times 10^6$		1.0102	$1 \times 10^6$
	1.0094	$1.5 \times 10^6$		1.0103	$1 \times 10^6$
	1.0095	$1 \times 10^6$		MC 1.01024	$4.2 \times 10^6$
			MC	1.0102	$1.4 \times 10^6$

TABLE I. Number of configurations generated on different lattice sizes. MC indicates multicanonical data. Simulations were performed in steps of  $10^{-4}$ .

method [37] to study the pseudo-critical points without noticeable extrapolation errors.

We have of course simulated the full U(1) group in double precision. We used two different programs to generate our configurations. One is an improved heatbath algorithm, the other one is capable of multicanonical updates (MC) combined with overrelaxation [38,24]. Both programs were tuned to yield acceptance rates of about 60%. The multicanonical algorithm was used in addition to the heatbath algorithm on  $12^4$  lattices. To produce the histogram needed for the multicanonical simulation we generated  $1.5 \cdot 10^5$  configurations using an overrelaxed Metropolis algorithm. For  $\beta = 1.01020$  the multicanonically reweighted histograms of the runs at  $\beta = 1.01024$  were used as the input. In all MC runs we used eight Metropolis updates followed by one overrelaxation step per link. A drastic reduction of the tunneling time is evident in figure 3. On smaller lattice sizes the heatbath algorithm is sufficient to generate statistics that allow a precise determination of all observables.

For safety reasons all results on our data sets were cross-checked with two independently developed evaluation programs. As a test of consistency we reweighted the multicanonical histogram to a coupling where we had heatbath data (see figure 4). Though we did not apply any smoothing algorithms to the histograms no relevant deviation can be observed.

To calculate the errors of our observables we proceeded as follows: We first divided our runs into five bins and calculated the error in each run by binning. The error for each lattice size was then calculated by a  $\chi^2$ -fit to a constant of all runs' binning results. In other words we did not recombine the histograms at the pseudo-critical points and used each run as an independent sample. Secondly we performed a jackknife error analysis in the same manner but with ten bins. The larger error was taken

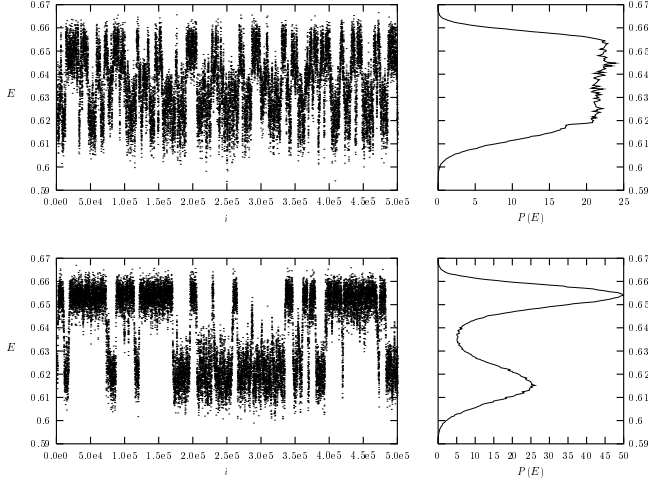


FIG. 3. The histories in multicanonical and heatbath simulations on a  $12^4$  lattice and the corresponding histograms normalized to unit area.

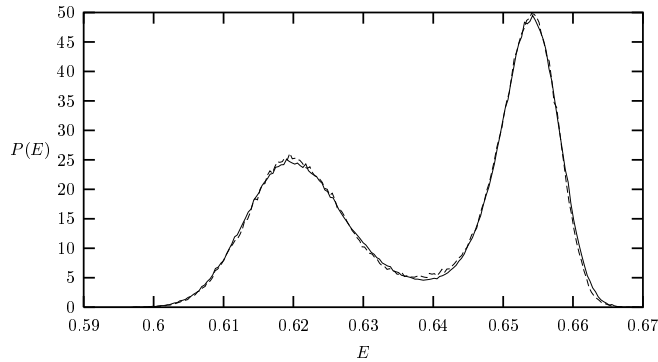


FIG. 4. The histograms in MC (solid) and heatbath simulations (dashed) on a  $12^4$  lattice.

$L$	$\beta_c(C_v)$	$C_{V,max} \times V^{-1}$	$\beta_c(\partial C_v/\partial\beta)$	$V^{-1}\partial C_v/\partial\beta$
4	0.9791(2)	.2205(5)E-02	0.9901(2)	.0803(8)
5	0.99466(5)	.1390(3)E-02	1.00035(6)	.101(1)
6	1.00172(4)	.955(3)E-03	1.00499(4)	.124(3)
7	1.00532(5)	.703(3)E-03	1.00735(5)	.150(7)
8	1.00744(4)	.551(4)E-03	1.00877(4)	.186(10)
9	1.00862(3)	.453(3)E-03	1.00951(3)	.230(14)
10	1.00939(5)	.382(4)E-03	1.01002(6)	.265(11)
12	1.010232(7)	.302(2)E-03	1.010567(8)	.429(5)
$L$	$\beta_c(U_2)$	$U_{2,min}$	$\beta_c(\partial U_2/\partial\beta)$	$V^{-1}\partial U_2/\partial\beta$
4	0.9764(2)	-.670(2)E-02	0.9882(2)	-.1574(15)E-03
5	0.99371(5)	-.3857(9)E-02	0.99961(6)	-.752(8)E-04
6	1.00132(4)	-.2525(7)E-02	1.00466(4)	-.423(9)E-04
7	1.00512(5)	-.1802(8)E-02	1.00719(5)	-.269(12)E-04
8	1.00734(4)	-.1387(9)E-02	1.00868(4)	-.191(10)E-04
9	1.00855(3)	-.1122(8)E-02	1.00945(3)	-.146(9)E-04
10	1.00935(5)	-.944(10)E-03	1.00998(6)	-.110(6)E-04
12	1.010217(6)	-.734(4)E-03	1.010553(7)	-.841(9)E-05
$L$	$\beta_c(U_4)$	$U_{4,min}$	$\beta_c(\partial U_4/\partial\beta)$	$V^{-1}\partial U_4/\partial\beta$
4	0.9753(2)	-.897(2)E-02	0.9870(2)	-.211(2)E-03
5	0.99327(5)	-.5158(11)E-02	0.99918(6)	-.1006(10)E-03
6	1.00111(4)	-.3372(10)E-02	1.00446(4)	-.565(12)E-04
7	1.00501(5)	-.2404(11)E-02	1.00708(5)	-.359(15)E-04
8	1.00728(4)	-.1851(12)E-02	1.00861(4)	-.255(13)E-04
9	1.00851(3)	-.1513(11)E-02	1.00941(3)	-.195(12)E-04
10	1.00932(5)	-.1254(14)E-02	1.00996(4)	-.148(9)E-04
12	1.010203(7)	-.979(6)E-03	1.010538(9)	-.1122(12)E-04

TABLE II. Pseudo-critical couplings and extrema of  $C_v, U_2, U_4$  and their derivatives as a function of the lattice size  $L$ .

into account. The jackknife error appeared to be usually larger, especially for the cumulants' derivatives, in heatbath data at all lattice sizes except  $L = 12$ . For  $L = 12$  the binning error was very large in heatbath data while no significant difference could be seen between the two methods in MC data. We interpret this phenomenon as a consequence of the lack of tunnelling events within a bin on a  $12^4$  lattice with a local heatbath algorithm. We observe just a few phase flips in  $10^5$  iterations. It is our experience that one needs at least a total of  $O(10^2)$  flips in order to control the statistical errors on the observables.

#### IV. MEASUREMENTS

The measurements of the standard cumulants and their derivatives are displayed in Table II for all the lattice sizes that we have studied and the results for the cumulants  $\kappa_n (3 \leq n \leq 6)$  are gathered in Table III.

It can be read from the tables that the statistical accuracy of the measurements of the pseudo-critical couplings and of the cumulants extrema has been improved by roughly one-order of magnitude with respect to previous studies. In particular the relative accuracy of our

$L$	$\beta_c(\kappa_3)$	$\kappa_3 \times V^{-2}$	$\beta_c(\kappa_4)$	$\kappa_4 \times V^{-3}$
4	0.9902(2)	-0.511(6)E-04	0.9983(2)	0.156(3)E-05
5	1.00035(6)	-0.264(3)E-04	1.00452(6)	0.659(9)E-06
6	1.00499(4)	-0.156(4)E-04	1.00737(5)	0.334(9)E-06
7	1.00735(5)	-0.102(5)E-04	1.00882(5)	0.191(9)E-06
8	1.00877(4)	-0.74(4)E-05	1.00973(4)	0.126(7)E-06
9	1.00951(3)	-0.57(4)E-05	1.01016(3)	0.90(6)E-07
10	1.01002(6)	-0.43(2)E-05	1.01048(6)	0.68(8)E-07
12	1.010564(9)	-0.338(4)E-05	1.010807(10)	0.460(7)E-07
$L$	$\beta_c(\kappa_5)$	$\kappa_5 \times V^{-4}$	$\beta_c(\kappa_6)$	$\kappa_6 \times V^{-5}$
4	0.9851(2)	0.385(7)E-06	0.9907(2)	-0.278(6)E-07
5	0.99827(6)	0.131(3)E-06	1.00110(6)	-0.770(13)E-08
6	1.00381(4)	0.55(2)E-07	1.00543(4)	-0.273(8)E-08
7	1.00663(5)	0.27(2)E-07	1.00764(5)	-0.117(6)E-08
8	1.00830(4)	0.162(13)E-07	1.00895(4)	-0.62(4)E-09
9	1.00919(3)	0.11(9)E-07	1.00964(3)	-0.38(3)E-09
10	1.00979(6)	0.71(8)E-08	1.01011(6)	-0.24(4)E-09
12	1.010446(8)	0.452(9)E-08	1.010611(9)	-0.137(3)E-09

TABLE III. Pseudo-critical couplings and extrema of  $\kappa_n$  cumulants as a function of the lattice size  $L$ .

results for the pseudo-critical couplings on the  $12^4$  lattice is now below  $10^{-5}$ , which is nearly comparable to the best results of numerical studies of lower-dimensional spin models.

In the following sections we shall present a finite-size scaling analysis of these results. But our analysis of corrections to scaling will be conventional and far from exhaustive. With our measurements given in raw form, without any interpretation, the reader has the possibility to do alternative analyses.

## V. PSEUDO-CRITICAL COUPLINGS

The pseudo-critical couplings are expected to follow the asymptotic finite-size scaling formula:

$$\beta_c(L) = \beta_c(\infty) + aL^{-\frac{1}{\nu}} \quad (27)$$

With data at eight lattice sizes it is possible to fit the three unknown parameters for each cumulant independently. With our statistics it is even possible to test the stability of the fits with respect to the lattice size. Table IV displays the results of such fits for the standard cumulants and their derivatives.

The fits are clearly not stable. The statistical errors are small enough to show the systematic decrease of the critical exponent  $\nu$  with the lattice size  $L$ . There is also a slight systematic decrease of the infinite-volume limit of the critical coupling  $\beta_c(\infty)$ . Moreover the fits are pretty consistent for all cumulants. Therefore we can try a combined fit to the pseudo-critical couplings of all standard cumulants and their derivatives, with a common value of  $\nu$  and  $\beta_c(\infty)$ . Such a fit is meaningful since these cumulants are defined in terms of algebraically independent

Cumulant	$L$	$\chi^2$	$\nu^{-1}$	a	$\beta_c(\infty)$
$C_v$	$L \geq 4$	2.42	2.999(17)	-2.091(56)	1.01145(3)
	$L \geq 5$	1.42	3.037(23)	-2.226(81)	1.01141(3)
	$L \geq 6$	0.731	3.111(46)	-2.54(21)	1.01135(5)
	$L \geq 7$	0.379	3.23(11)	-3.17(65)	1.01128(7)
$U_2$	$L \geq 4$	1.29	3.090(16)	-2.554(64)	1.01140(2)
	$L \geq 5$	1.04	3.112(22)	-2.648(92)	1.01138(3)
	$L \geq 6$	0.829	3.161(44)	-2.89(23)	1.01134(4)
	$L \geq 7$	0.704	3.26(11)	-3.48(68)	1.01128(7)
$U_4$	$L \geq 4$	1.24	3.116(16)	-2.727(67)	1.01139(2)
	$L \geq 5$	1.08	3.136(21)	-2.818(97)	1.01137(3)
	$L \geq 6$	0.878	3.184(43)	-3.07(24)	1.01133(4)
	$L \geq 7$	0.816	3.28(11)	-3.66(71)	1.01127(7)
$\frac{\partial C_v}{\partial \beta}$	$L \geq 4$	1.43	3.012(26)	-1.398(58)	1.01136(3)
	$L \geq 5$	1.01	3.057(37)	-1.509(91)	1.01133(3)
	$L \geq 6$	0.715	3.140(71)	-1.75(22)	1.01128(5)
	$L \geq 7$	0.730	3.26(17)	-2.22(72)	1.01123(7)
$\frac{\partial U_2}{\partial \beta}$	$L \geq 4$	1.12	3.096(24)	-1.705(66)	1.01133(2)
	$L \geq 5$	0.836	3.133(35)	-1.81(11)	1.01131(3)
	$L \geq 6$	0.704	3.196(67)	-2.03(24)	1.01128(4)
	$L \geq 7$	0.898	3.28(16)	-2.37(73)	1.01124(7)
$\frac{\partial U_4}{\partial \beta}$	$L \geq 4$	0.724	3.142(24)	-1.904(71)	1.01131(3)
	$L \geq 5$	0.687	3.165(34)	-1.98(11)	1.01130(3)
	$L \geq 6$	0.613	3.218(66)	-2.18(26)	1.01127(4)
	$L \geq 7$	0.732	3.30(16)	-2.57(77)	1.01123(7)

TABLE IV. Independent second-order finite-size scaling fits to the pseudo-critical couplings of standard cumulants and their derivatives.

combinations of the moments of the plaquette energy distribution. We can also test the stability of this combined fit with respect to the lattice size. The parameters of these fits are given in Table V. Fig. 5 displays the result of the combined fit to the  $L \geq 6$  data points. Errors on the data points are much smaller than the marker sizes.

We can repeat the same kind of analysis for the energy cumulants  $\kappa_n$ . The independent fits are shown in Table VI and the combined fits in Table VII. The result of the combined fit to the  $L \geq 6$  data points is also displayed in Fig. 6.

The critical values of  $\nu$  and  $\beta_c(\infty)$  extracted from the cumulants  $\kappa_n$  are very similar to those extracted from the standard cumulants or their derivatives. Studying

$L$	$\chi^2$	$\beta_c(\infty)$	$\nu^{-1}$
$L \geq 4$	5.86	1.011348(8)	3.1059(72)
$L \geq 5$	4.09	1.011317(10)	3.144(10)
$L \geq 6$	1.81	1.011269(14)	3.222(19)
$L \geq 7$	0.692	1.011224(19)	3.329(35)
$L \geq 8$	0.799	1.011235(29)	3.304(62)
$L \geq 9$	0.872E-01	1.011206(43)	3.4249(69)

TABLE V. Combined asymptotic finite-size scaling fits to the pseudo-critical couplings of the cumulants  $C_v$ ,  $U_2$ ,  $U_4$ ,  $\frac{\partial C_v}{\partial \beta}$ ,  $\frac{\partial U_2}{\partial \beta}$  and  $\frac{\partial U_4}{\partial \beta}$ .

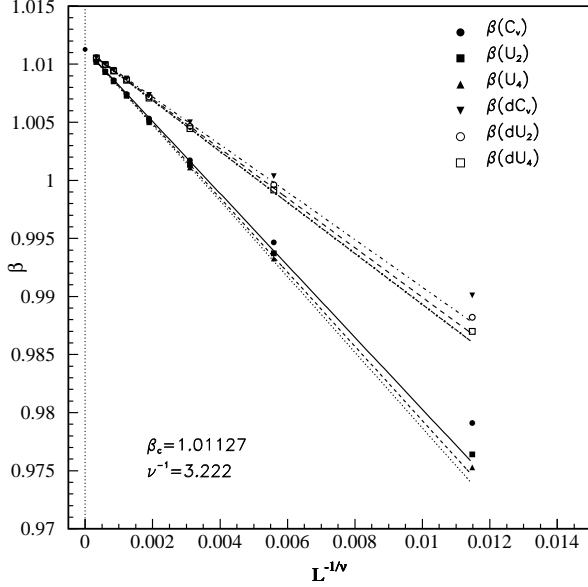


FIG. 5. Combined fit to the  $L \geq 6$  data points of the pseudo-critical couplings of the standard cumulants and their derivatives.

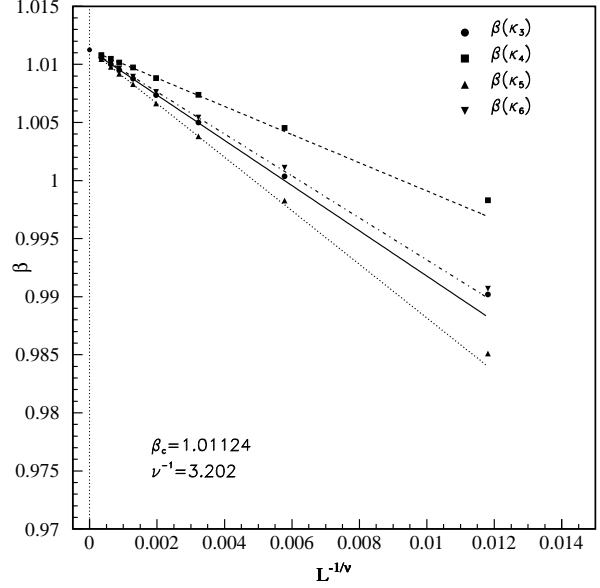


FIG. 6. Combined fit to the  $L \geq 6$  data points of the pseudo-critical couplings of the cumulants  $\kappa_n$ .

Cumulant	$L$	$\chi^2$	$\nu^{-1}$	a	$\beta_c(\infty)$
$\kappa_3$	$L \geq 4$	1.72	3.005(27)	-1.381(58)	1.01136(3)
	$L \geq 5$	1.05	3.060(38)	-1.515(92)	1.01132(3)
	$L \geq 6$	0.720	3.146(72)	-1.77(23)	1.01128(5)
	$L \geq 7$	0.711	3.28(17)	-2.26(74)	1.01122(7)
$\kappa_4$	$L \geq 4$	1.18	3.011(44)	-0.858(60)	1.01129(3)
	$L \geq 5$	0.872	3.078(62)	-0.959(97)	1.01127(3)
	$L \geq 6$	0.724	3.20(13)	-1.19(27)	1.01123(5)
	$L \geq 7$	0.812	3.38(28)	-1.69(93)	1.01119(7)
$\kappa_5$	$L \geq 4$	1.02	3.083(22)	-1.876(65)	1.01133(3)
	$L \geq 5$	1.08	3.063(31)	-1.815(92)	1.01134(3)
	$L \geq 6$	0.684	3.139(60)	-2.08(22)	1.01130(5)
	$L \geq 7$	0.721	3.24(15)	-2.51(68)	1.01125(8)
$\kappa_6$	$L \geq 4$	0.843	3.103(28)	-1.512(67)	1.01129(3)
	$L \geq 5$	0.887	3.079(40)	-1.454(95)	1.01130(3)
	$L \geq 6$	0.485	3.174(77)	-1.72(24)	1.01126(5)
	$L \geq 7$	0.489	3.29(19)	-2.137(64)	1.01122(7)

TABLE VI. Independent second-order finite-size scaling fits to the pseudo-critical couplings of the  $\kappa_n$  cumulants.

$L$	$\chi^2$	$\beta_c(\infty)$	$\nu^{-1}$
$L \geq 4$	2.41	1.011299(12)	3.084(14)
$L \geq 5$	1.59	1.011288(13)	3.105(18)
$L \geq 6$	0.718	1.011244(17)	3.202(31)
$L \geq 7$	0.442	1.011206(25)	3.319(63)
$L \geq 8$	0.564	1.011220(37)	3.27(11)
$L \geq 9$	0.856E-02	1.011191(53)	3.429(14)

TABLE VII. Combined asymptotic finite-size scaling fits to the pseudo-critical couplings of the cumulants  $\kappa_3$ ,  $\kappa_4$ ,  $\kappa_5$  and  $\kappa_6$ .

the pseudo-critical couplings of the cumulants  $\kappa_n$  does not bring any significant improvement over the standard cumulants. The pseudo-critical couplings are not very sensitive to the corrections to asymptotic scaling. Even if the finite-size scaling violations are clearly visible on Figs. 5 and 6 at the small lattice sizes  $L = 4$  or  $5$ , it would not be possible to introduce additional parameters in the fits.

## VI. CUMULANTS' EXTREMA

In this section we will present some selected analyses of the finite size scaling behaviour of the cumulants we calculated. As the main result we can state that the finite-size scaling behavior of all cumulants is consistent with a first-order transition. However we observe a difference in the corrections to scaling of the specific heat and the Binder cumulant on one hand and their derivatives and the energy cumulants on the other hand. Up to the lattice sizes we calculated the first do not follow yet the expected pattern in a first order phase transition while the other show a clear first order behaviour. To demonstrate this we will present selected fits to our data. In all pictures in the following subsections the solid curves denote the fit to the ansatz which yields the best results.

### A. Asymptotic scaling

It is certainly not possible to describe the data without taking into account the corrections to scaling. However



$L$	$C_v$	$U_4$	$\frac{\partial C_v}{\partial \beta}$	$\frac{\partial U_4}{\partial \beta}$
9	3.299(17)	3.250(17)	3.467(56)	3.402(63)
8	3.177(28)	3.132(27)	3.19(11)	3.19(12)
7	3.121(16)	3.070(17)	3.23(11)	3.183(97)
6	3.030(12)	2.942(12)	3.123(64)	3.064(59)
5	2.983(7)	2.856(7)	3.050(36)	2.962(32)
4	2.968(5)	2.788(5)	3.016(18)	2.906(16)
$L$	$\kappa_3$	$\kappa_4$	$\kappa_5$	$\kappa_6$
9	3.479(63)	3.422(57)	3.405(55)	3.416(47)
8	3.19(11)	3.30(13)	3.27(12)	3.30(11)
7	3.22(12)	3.247(80)	3.282(90)	3.246(62)
6	3.125(66)	3.139(51)	3.135(59)	3.126(39)
5	3.048(38)	3.075(30)	3.055(36)	3.061(22)
4	3.019(20)	3.046(20)	3.038(18)	3.045(15)

TABLE VIII. Critical exponent  $\nu^{-1}$  extracted from lattice sizes  $L$ ,  $L + 1$  and  $L + 2$  for each cumulant extremum with the ansatz *FSS2a*.

it is instructive to define, for any cumulant  $\kappa$ , an "effective critical exponent"  $\nu_\kappa(L)$  by fitting the data at scales  $L$ ,  $L + 1$  and  $L + 2$  to the asymptotic form of the scaling ansätze of sect. II:

$$FSS2a : \quad \kappa(L) = bL^\tau \quad (28)$$

We shall refer to this ansatz as *FSS2a*. The relation between the critical exponents  $\tau$  and  $\nu$  depends of course upon the cumulant. The results are displayed in Table VIII.

We observe again in Table VIII a systematic decrease of the critical exponent  $\nu$  with the lattice size  $L$ . The effective critical exponent  $\nu(L)$  is pretty consistent at each scale  $L$  across the cumulants  $\kappa_n$  and with the values found in the combined fits of the pseudo-critical couplings. There is however some dispersion among the standard cumulants and their derivatives not observed in the analysis of pseudo-critical couplings. In fact the  $\chi^2$  of these asymptotic fits is quite high even with 2 parameters and only 3 data points. We see here a first manifestation of the expected improved scaling behavior of the energy cumulants  $\kappa_n$ .

## B. Corrections to scaling

The asymptotic scaling fits for the cumulants' extrema as well as for the pseudo-critical couplings hint at a first-order transition. Our working hypothesis will be to describe the data with scaling corrections to a first-order transition. These corrections are expected to be expressible as a series expansion in the inverse volume  $V^{-1}$ . Since we limit ourselves to three-parameter fits, we shall introduce the two fitting ansätze:

$$FSS1a : \quad \kappa(L) \times V^{-k} = a + bL^{-d} \quad (29)$$

$$FSS1b : \quad \kappa(L) \times V^{-k} = a + bL^{-d} + cL^{-2d} \quad (30)$$

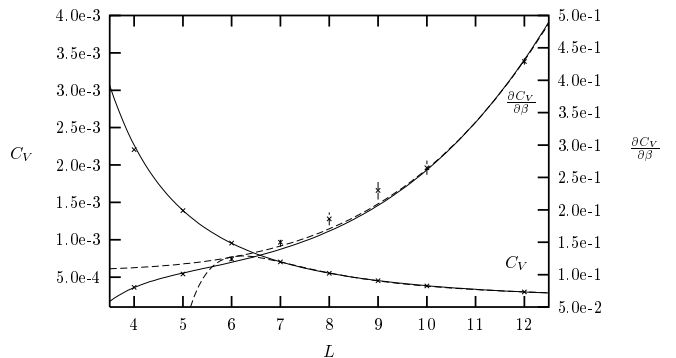


FIG. 7. Fits to the specific heat and its derivative.

The volume normalization factor is chosen such that the fitting ansatz makes sense. With the definitions of sect. II we have  $k = 0$  for  $U_2$  and  $U_4$ ,  $k = 1$  for  $C_v$ ,  $\frac{\partial U_2}{\partial \beta}$ ,  $\frac{\partial U_4}{\partial \beta}$ ,  $k = 2$  for  $\frac{\partial C_v}{\partial \beta}$  and  $k = n - 1$  for  $\kappa_n$ .

We shall need another, more phenomenological fitting ansatz:

$$FSS2b : \quad \kappa(L) \times V^{-k} = a + bL^{-\omega} \quad (31)$$

The volume normalization factor  $V^{-k}$  is by definition the same as for the first-order fitting ansätze. Therefore the exponent  $\omega$  parameterizes the corrections to an asymptotic first-order behaviour. Introducing such an effective exponent allows a more flexible description of the corrections. One should find that  $\omega \rightarrow d$  when we reach the asymptotic regime.

The best *FSS1b* fit to the specific heat is represented by the dashed line in Fig. 7. Obviously it cannot describe the smallest lattice sizes. On the other hand the fitting ansatz *FSS2b* describes our data on the specific heat perfectly. Our data on  $\partial C_v/\partial \beta$  have the largest errors of all the results we produced. Thus the quality of the best fits with *FSS1b* (solid line) or *FSS1a* (dashed line) is not good.

The ansatz *FSS2b* is also able to reproduce the data on the Binder cumulant quite accurately (solid line in Fig. 8). We observe again that ansatz *FSS1b* (dashed line) fails to reproduce the smallest lattice sizes. The description of the derivative  $\partial U_4/\partial \beta$  by *FSS1b* (solid line) is much better and *FSS1a* gives already a good fit for all but the smallest lattice sizes (dashed line). The results for  $U_2$  and its derivative are quite similar to  $U_4$  and its derivative and will not be reproduced here.

In the same way we find that the first-order ansätze can fit the data on the energy cumulants  $\kappa_n$ . In Fig. 9 all solid lines represent the best fits with ansatz *FSS1b* whereas all dashed lines represent the best fits with ansatz *FSS1a*. The cumulant  $\kappa_4$  is a noticeable exception. The asymptotic first-order ansatz *FSS1a* is already able to describe all data points and is nearly indistinguishable from ansatz *FSS1b*. We have another, and more vivid manifestation of the improved scaling behaviour of the energy cumulants  $\kappa_n$ .

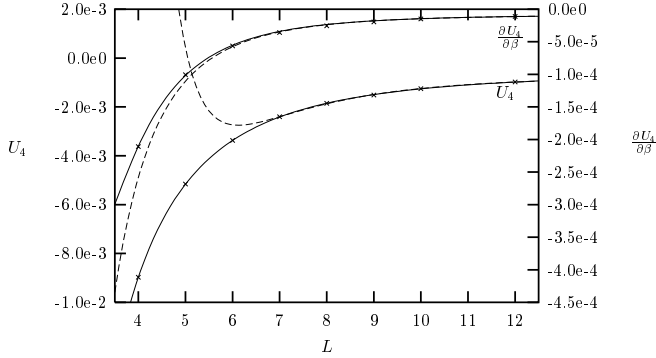


FIG. 8. Fits to the Binder Cumulant and its derivative.

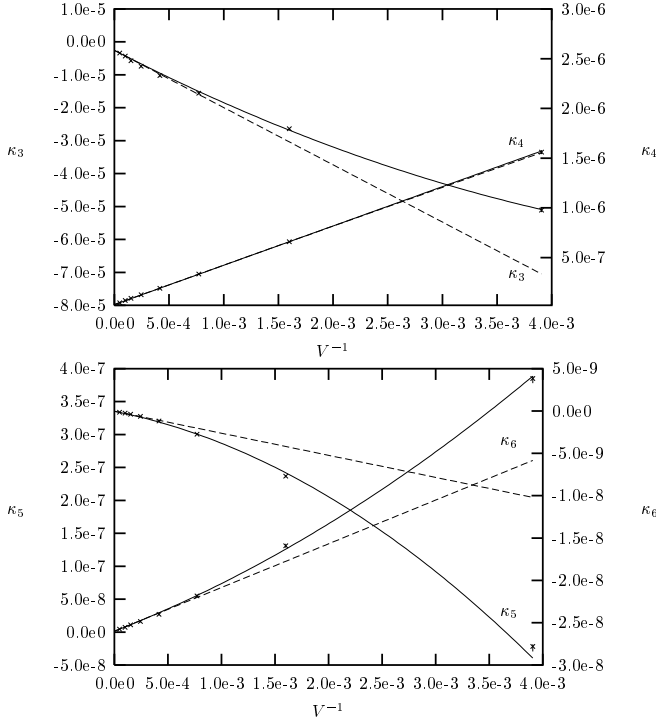


FIG. 9. Fits to the energy cumulants  $\kappa_n$ .

Cum.	Fit	$L$	$\chi^2$	a	b
$C_v$	FSS2b	$L \geq 5$	0.52	.147(6)E-03	.580(23)E-01
$\frac{\partial C_v}{\partial \beta}$	FSS1b	$L \geq 5$	0.58	.149(4)E-04	.121(5)
$U_4$	FSS2b	$L \geq 4$	0.85	-.545(11)E-03	-.352(7)
$\frac{\partial U_4}{\partial \beta}$	FSS1b	$L \geq 4$	1.79	-.823(14)E-05	-.632(11)E-01
$\kappa_3$	FSS1b	$L \geq 5$	0.50	-.244(6)E-05	-.196(9)E-01
$\kappa_4$	FSS1a	$L \geq 4$	0.94E-01	-.270(8)E-07	-.395(5)E-03
$\kappa_5$	FSS1b	$L \geq 4$	1.26	.143(15)E-08	.631(22)E-04
$\kappa_6$	FSS1b	$L \geq 5$	0.43	-.334(71)E-10	-.206(13)E-05

TABLE IX. Best fits to the cumulants' extrema.

Table IX gives a quantitative content to the previous qualitative observations. This table contains the parameters  $a$  and  $b$  of the best fits displayed in the figures. We always choose the smallest lattice size with a  $\chi^2$  per degree of freedom less than 2.

The main feature is the smallness of the ratios  $\frac{a}{b}$ . In the first-order fits, the leading contribution  $a$  is generally smaller than the correction term  $bL^{-d}$  up to the lattice size  $L = 12$ . It is no surprise that the first-order nature of the transition is so difficult to observe.

We can get order-of-magnitude estimates of the parameters of a first-order transition by comparing the values of  $a$  with the predictions of the (very crude) double-gaussian approximation [29]. The height of the maximum of the specific heat should increase linearly with  $L^d$  as:

$$C_{v,max} = V \frac{3\beta_c^2}{2} (e_o - e_d)^2 + O(1) \quad (32)$$

where  $\beta_c$  is the infinite-volume critical coupling and  $e_o - e_d$  is the latent heat. We find

$$e_o - e_d \approx 0.029 \quad (33)$$

The minimum of the Binder cumulant is predicted to be [30,31]:

$$U_{4,min} = -\frac{(e_o^2 - e_d^2)^2}{12(e_o e_d)^2} + O(V^{-1}) \quad (34)$$

We get another estimate of the latent heat which agrees pretty well with (33):

$$e_o - e_d \approx 0.026 \quad (35)$$

## VII. CONCLUSION

Our study shows that finite-size scaling violations are indeed present in each observable for lattice sizes  $4 \leq L \leq 12$ . The observed scaling violations are consistent for all observables: the critical exponent  $\nu$  systematically **decreases** with the lattice size  $L$ . Asymptotic finite-size scaling of all cumulants and of their pseudo-critical

couplings yields consistently  $\nu \approx 0.29$  for  $L \geq 9$  which points towards a first-order transition.

The scaling violations in the pseudo-critical couplings and the cumulant values decrease slowly with the lattice size. This slow variation, which is hard to unravel, can explain the claims for a second-order transition with  $\nu \approx 0.33$ . However the scaling violations seem to decrease more rapidly for the derivatives of the standard cumulants and for the cumulants  $\kappa_n$ . The finite-size behavior of all these cumulants can be completely described in the range  $4 \leq L \leq 12$  by volume correction terms of order  $V^{-1}$  and  $V^{-2}$ . The cumulant  $\kappa_4$  is even completely described by the asymptotic first-order formula.

There seems to be a correlation between the amount of scaling violations in each cumulant extremum and the location of its pseudo-critical-coupling. The closer the pseudo-critical coupling is, at fixed lattice size, from the infinite-volume critical point, the better the description of the extremum by a first-order transition. All the cumulants we have studied follow this rule. Then we can make two observations.

On the one hand, if we had chosen to study the extremum in each cumulant which is farthest from  $\beta_c(\infty)$  we would certainly have found a behavior inconsistent with a first-order transition and concluded to a second-order transition with a critical exponent  $\nu$  *greater* than 0.33. We suggest that this is the origin of many claims for a large critical exponent  $\nu$ . Most of them are not based on finite-size scaling analyses of the standard cumulants, which all should give  $\nu \leq 0.33$ , but come from various analyses done at couplings  $\beta$  smaller than  $\beta_{C_v}(L)$ , the pseudo-critical coupling of the specific heat in the corresponding lattices.

On the other hand we could think of studying still higher-order  $\kappa_n$  cumulants to get closer to  $\beta_c(\infty)$ . However we would face two difficulties. First the statistical noise increases with  $n$ . Secondly the extrapolation from the couplings where we generated our configurations gets large. The solution might be to generate the configurations for all lattice sizes at the infinite-volume critical point and use the method developed [32,33] for the study of first-order transitions in Potts models.

However it is not clear how the proofs can be extended to the case of the U(1) phase transition. Potts models have a discrete symmetry and a local order parameter whereas the U(1) lattice gauge theory has a continuous local symmetry and a non-local order parameter since the proof of existence of the phase transition uses the Wilson criterion [37]. In Potts models the physical correlation lengths in both pure phases stay finite in the infinite volume limit whereas there exist massless photons in the ordered phase of U(1). Clearly the U(1) lattice gauge theory deserves as much numerical study as the lower-dimensional spin models and theoretical understanding of the scaling violations will be required before a definitive conclusion on the nature of its phase transition.

## ACKNOWLEDGMENTS

One of us (C.R.) is grateful to the Freie Universität Berlin for its hospitality during a visit when this manuscript was completed and acknowledges a financial support by the Graduiertenkolleg "Strukturuntersuchungen, Präzisionstests und Erweiterungen des Standardmodells der Elementarteilchenphysik".

B. K. wants to thank P. E. L. Rakow from DESY-IfH Zeuthen for his support during the preparation of the diploma thesis. He initialized the investigation of the latent heat.

- 
- [1] M. Creutz, L. Jacobs and C. Rebbi, Phys. Rev. **D20**, (1979) 1915.
  - [2] J. Fröhlich and T. Spencer, Commun. Math. Phys. **83** (1982) 411.
  - [3] B. Lautrup and M. Nauenberg, Phys. Lett. **B95** (1980) 63.
  - [4] J. Jersák, T. Neuhaus and P.M. Zerwas, Phys. Lett. **133B** (1983) 103.
  - [5] R. Gupta, M.A. Novotny and R. Cordery, Phys. Lett. **B172** (1986) 86.
  - [6] A. N. Burkitt, Nucl. Phys. **B270** [FS16] (1986) 575.
  - [7] C. B Lang, Nucl. Phys. **B280** [FS18] (1987) 255.
  - [8] C.B. Lang and C. Rebbi, Phys. Rev. **D35** (1987) 2510.
  - [9] K. Decker, A. Hasenfratz and P. Hasenfratz, Nucl. Phys. **B295** [FS21] (1988) 21.
  - [10] H.G. Evertz, J. Jersák, T. Neuhaus and P.M. Zerwas, Nucl. Phys. **B251** [FS13] (1985) 279.
  - [11] J. Jersák, T. Neuhaus and P.M. Zerwas, Nucl. Phys. **B251** [FS13] (1985) 299.
  - [12] G. Bhanot, T. Lippert, K. Schilling and P. Ueberholz, Nucl. Phys. **B378**, (1992) 633.
  - [13] T. DeGrand and D. Toussaint, Phys. Rev. **D22** (1980) 2478.
  - [14] J.S. Barber, Phys. Lett. **B147** (1984) 330.
  - [15] J.S. Barber, R.E. Shrock and R. Schrader, Phys. Lett. **B152** (1985) 221.
  - [16] J.S. Barber and R.E. Shrock, Nucl. Phys. **B257** (1985) 515.
  - [17] W. Kerler, C. Rebbi and A. Weber, Phys. Rev. **D50** (1994) 6984; Nucl. Phys. **B450** (1995) 452; Phys. Lett. **B348** (1995) 565; Phys. Lett. **B380** (1996) 346.
  - [18] W. Kerler, C. Rebbi and A. Weber, Phys. Lett. **B392** (1997) 438.
  - [19] G. Damm and W. Kerler, HUB-EP-97/63 (1997), hep-lat/9709061.
  - [20] C.B Lang and T. Neuhaus, Nucl. Phys. **B431**, (1994) 119.
  - [21] J. Jersák, C.B Lang and T. Neuhaus, Phys. Rev. Lett. **77** (1996) 1933.
  - [22] J. Jersák, C.B Lang and T. Neuhaus, Phys. Rev. **D54** (1996) 6909.

- [23] J. Cox, W. Franzki, J. Jersák, C.B. Lang, T. Neuhaus, A. Seyfried, P. W. Stephenson, Nucl. Phys. **B499** (1997) 371.
- [24] B. Klaus, Diploma thesis (FU Berlin, 1995).
- [25] C. Roiesnel, Phys. Lett. **B405** (1997) 126.
- [26] M.E. Fisher, in Critical phenomena, Proc. 51st Enrico Fermi Summer School, Varena, ed. M.S. Green (Academic Press, NY, 1972).
- [27] V. Privman, P.C. Hohenberg and A. Aharony, *Phase Transitions and Critical Phenomena* (ed. C. Domb and J.L. Lebowitz), Vol. 14, p. 1, Academic Press, (1991) London.
- [28] M.E.Fischer and N. Berker, Phys. Rev. **B26** (1982) 2507.
- [29] M.S. Challa, D.P. Landau, K. Binder, Phys. Rev. **B34** (1986) 1841;
- [30] A. Billoire, R. Lacaze, A. Morel, S. Gupta, A. Irbäck and B. Petersson, Phys. Rev. **42** (1990) 6743.
- [31] J. Lee and J.M. Kosterlitz, Phys. Rev. **B43** (1991) 3625.
- [32] C. Borgs and R. Kotecky, J. Stat. Phys. **61** (1990) 79;
- [33] C. Borgs, R. Kotecky, and S. Miracle-Solé, J. Stat. Phys. **62** (1991) 529.
- [34] A. Billoire, T. Neuhaus and B. Berg, Nucl. Phys. **B413** (1994) 795.
- [35] K. Binder, Z. Phys. B **43** (1981) 119.
- [36] W. Janke and S. Kappler, J. Phys. I (France) **7** (1997) 663.
- [37] A.M. Ferrenberg and R.H. Swendsen, Phys. Rev. Lett. **61**, (1988) 2635; **63** (1989) 1658; **63** (1989) 1195.
- [38] B. Berg and T.Neuhaus, Phys. Lett. **B267** (1991) 249; Phys. Rev. Lett. **68** (1992) 9.